AIAA JOURNAL
Vol. 36, No. 1, January 1998

Effect of Ply Thickness on Fracture of Notched Composite Laminates

Rajesh S. Vaidya,* J. C. Klug,* and C. T. Sun†
Purdue University, West Lafayette, Indiana 47907-1282

The effect of ply thickness on unnotched and notched strength of fiber-dominated laminates is investigated. Experiments are conducted to examine the effect of subcritical damage on fracture toughness of AS4/3501-6 graphite/epoxy laminates with cross-ply and quasi-isotropic configurations. It is observed that ply thickness has a significant effect on the notched behavior of cross-ply laminates but less so for quasi-isotropic laminates. The experimentally observed crack-tip damage in the form of axial splitting in the 0-deg plies and delamination is modeled by a two-dimensional finite element analysis using Mindlin plates, and the criterion that controls damage (split) growth is established. The role of such damage on crack-tip stress distribution is investigated, and inferences are drawn to determine the circumstances under which a fracture mechanics type of failure model can be used to predict the notched response of these laminates.

Introduction

COMPOSITE materials are notch sensitive. The presence of cracklike or damage defects in structural components may drastically reduce their load carrying capacity. For this reason, the study of notched response of composites in the presence of stress enhancers such as cracks has been an important research area in the composites community.

A vast amount of experimental literature is available on the notched response of different composite material systems. Detailed studies have been carried out to examine the evolution of crack-tip damage and eventual failure of notched composite systems. Several strength-based and fracture-mechanics-based models have also been proposed to predict the failure stress of such laminates under uniaxial tensile loading. However, there is still no consensus on a single model that can successfully predict failure of all types of laminates. This is because subcritical crack-tip damage, which plays a very important role in determining the eventual failure load of the laminate, often varies with laminate configuration. It is important to understand the role of such damage on crack-tip stress distribution and eventual failure to determine which type of model would work well for a given laminate configuration.

In a previous paper, a fracture criterion was proposed to predict the failure of fiber-dominated laminates containing through thickness cracks.[1] The layup-independent criterion was based on determining a material parameter K_Q^0 that characterized the fracture toughness of the principal load bearing ply (0-deg ply). The parameter K_Q^0 represents the in situ fracture toughness of a notched 0-deg layer in a laminate. Once its value is established from a specific laminate, it can be used to predict fracture toughness of other laminates of the same material system. It was demonstrated that the model works well for fiber-dominated laminates with well-dispersed plies under mode I and mixed-mode loading conditions. However, the material parameter was determined from tests on laminates with standard ply thickness and did not account for changes in toughness with thickness of the plies.

Some researchers have found that thickness of the plies plays a significant role in failure of notched laminates.[2] It was reported that clustered laminates of a cross-ply configuration had higher toughness than well-dispersed laminates containing the same proportion of 0- and 90-deg plies. The reason was attributed to the larger crack-tip damage zone observed in the clustered laminates. Kortschot and Beaumont,[3,4] Kortschot et al.,[5] and Kortschot and Beaumont[6] studied the effect of damage zone size on fracture strength of cross-ply laminates and modeled the damage using finite element analysis. They suggested that the critical damage zone size is an important criterion in determining laminate strength and presented a strength-based criterion to predict failure stress based on damage size. Several other experimental studies have also examined the role of crack-tip damage on notched strength of composite laminates.[7–9] The consensus derived from these studies is that crack-tip damage in the form of matrix cracking and delamination reduces the strength of the crack-tip stress concentration and elevates fracture strength.

The present study investigates the effect of ply thickness on crack-tip damage and failure of cross-ply and quasi-isotropic laminate configurations. The primary objective is to examine the role of ply thickness on laminate notch sensitivity and determine which laminates lie outside (or inside) the framework of the fracture-mechanics-based criterion.[1]

A finite element analysis is also performed to study the effect of crack-tip damage on the stress distribution in the principal load bearing plies. The principal damage mechanisms observed from the experimental study are modeled in the analysis, and a strain-energy-based criterion for growth of damage is presented. This criterion can provide an estimate of the damage zone size of different laminate configurations. Finally, a parametric study is conducted for different laminate configurations to determine which laminates are likely to exhibit large damage zones.

Experimental Procedure

The laminate configurations used for the study of ply thickness effect are listed in Table 1. The material system used was AS4/3501-6 graphite epoxy composite with a nominal ply thickness of 0.127 mm. Different effective ply thickness values were achieved by varying the parameter n (see Table 1). The test specimens were cut from 30.5 × 30.5 cm panels using a waterjet. The specimen dimensions were 25.4 × 3.81 cm with 3.81-cm-long end tabs. To make the cracks, a starter hole was first drilled in the laminate to minimize any delamination caused by the waterjet. The crack was then introduced by a waterjet cut and further extended by a 0.2-mm-wide jeweler's saw blade.

The quasistatic experiments were conducted under position control at a head displacement rate of 0.254 mm/min on a servo-hydraulically driven MTS machine. The load and displacement were recorded using a personal computer-based data acquisition system. Crack-tip damage evolution was monitored by diiodobutane enhanced x-ray examination at different load levels. The fractured specimens were also examined to determine the failure mode of the laminates.

Received Feb. 3, 1997; revision received Aug. 12, 1997; accepted for publication Aug. 27, 1997.

*Graduate Student, School of Aeronautics and Astronautics.
†Professor, School of Aeronautics and Astronautics. Fellow AIAA.

Table 1 Laminate configurations used to study ply thickness effect

Laminate configuration	Number of repeating plies
$[90_n/0_n/90_n/0_n/90_n]$	$n = 1, 2, 3, 4$
$[0_n/90_n]_{2s}$	$n = 1, 2$
$[0_n/90_n]_s$	$n = 2, 4$
$[0_n/90_n/45_n/-45_n]_s$	$n = 1, 2, 4$

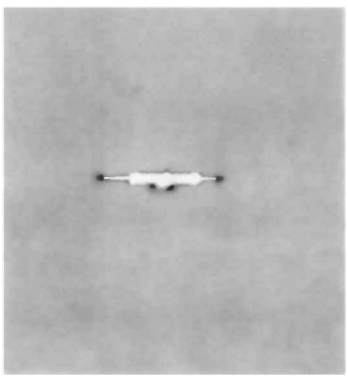

Fig. 1 Crack-tip damage in [90/0/90/0/90] laminate at 82% of failure load.

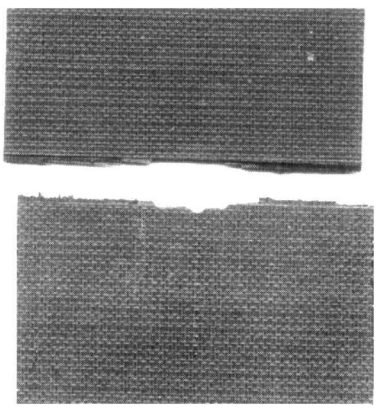

Fig. 2 Failure mode of [90/0/90/0/90] laminate.

Effect of Ply Thickness on Notched Strength

Cross-Ply Laminate Configurations

The $[90_n/0_n/90_n/0_n/90_n]$ laminate configuration has the 0-deg layer constrained between adjacent 90-deg layers. This provides an additional degree of constraint compared to the case where the 0-deg layer is on the surface. For $n = 1$, which corresponds to single-ply thickness, this laminate shows very limited crack-tip damage even at 82% of the failure load (Fig. 1). This damage appears in the form of matrix cracks in the 0- and 90-deg layers along their respective fiber directions. Final failure of this laminate occurs by fiber breakage of the 0-deg plies along the plane of the original notch (Fig. 2). Doubling the effective ply thickness in this laminate ($n = 2$) has a significant effect on the crack-tip damage. Extensive damage is observed in the form of transverse matrix cracking, axial splitting (matrix cracks in the 0-deg layer) and delamination (Fig. 3). This laminate also fails by fiber breakage in the 0-deg layer initiating from the tip of the notch. For $n = 3$ and 4, the damage zone is even larger (Fig. 4), and laminate failure is caused by free edge-induced fiber breakage. The failure of these thicker laminates is no longer crack dominated; instead it is controlled by free edge failure.

A comparison of the unnotched and notched strengths of these laminates reveals that, whereas ply thickness has little effect on unnotched strength, the notched strength is significantly affected (Figs. 5 and 6). The notched strength increases with increasing ply

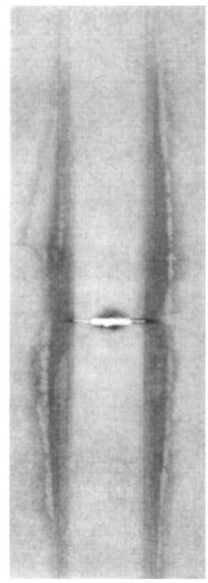

Fig. 3 Damage in $[90_2/0_2/90_2/0_2/90_2]$ laminate at 96% of failure.

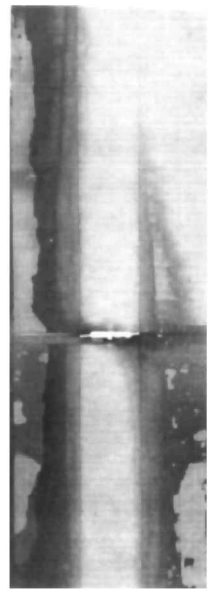

Fig. 4 Damage in $[90_3/0_3/90_3/0_3/90_3]$ laminate at 97% of failure.

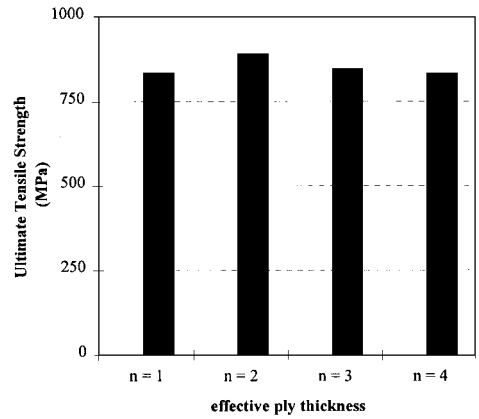

Fig. 5 Unnotched strength of $[90_n/0_n/90_n/0_n/90_n]$ laminates.

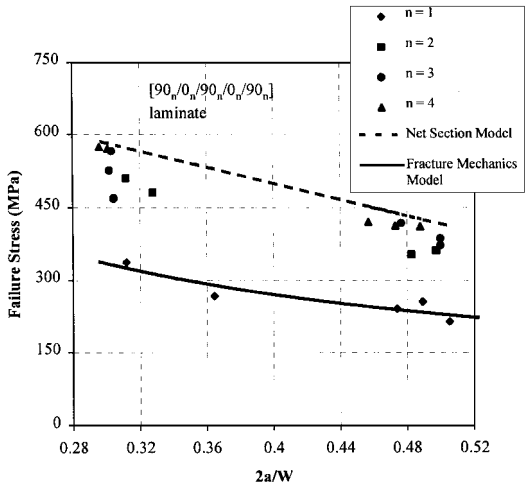

Fig. 6 Failure stress vs flaw size for $[90_n/0_n/90_n/0_n/90_n]$ laminate.

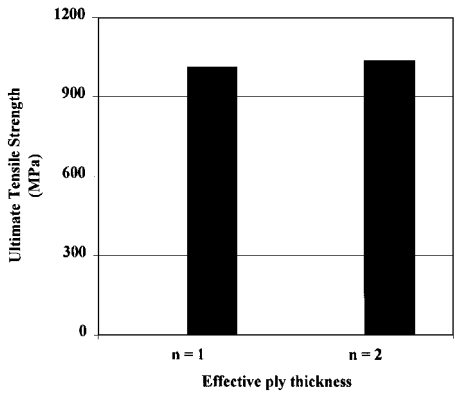

Fig. 7 Unnotched strength of $[0_n/90_n]_{2s}$ laminates.

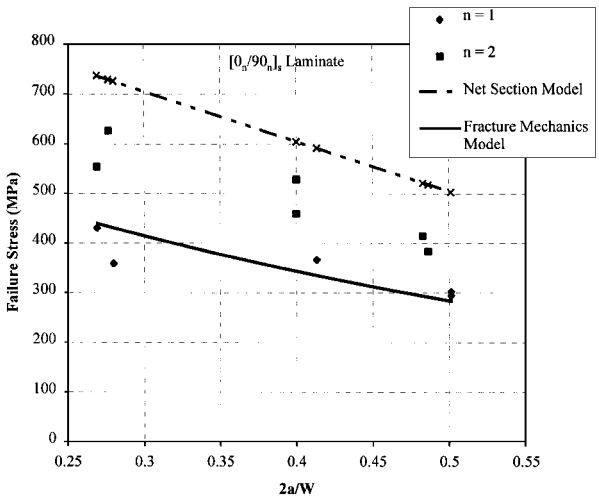

Fig. 8 Failure stress vs flaw size for $[0_n/90_n]_{2s}$ laminates.

thickness, and there is a transition of failure modes from a crack-dominated failure to a free edge-induced failure. In the latter failure mode, the laminates approach their theoretical net-section strength defined as

$$\sigma_N^{\infty} = \sigma_{\mathrm{UTS}}[1 - (2a/W)] \tag{1}$$

where σ_{UTS} is the ultimate strength of the laminate, $2a$ is the crack length, and W is the specimen width.

The $[0_n/90_n]_{2s}$ laminate shows a similar ply thickness effect (Figs. 7 and 8). The unnotched strength of the laminate seems

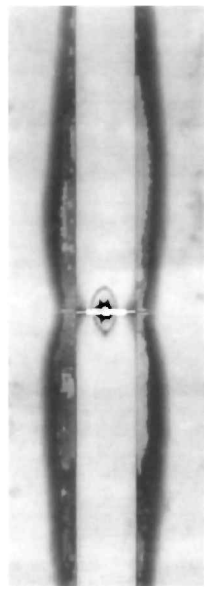

Fig. 9 Damage in $[0_2/90_2]_s$ laminate at 95% of failure load.

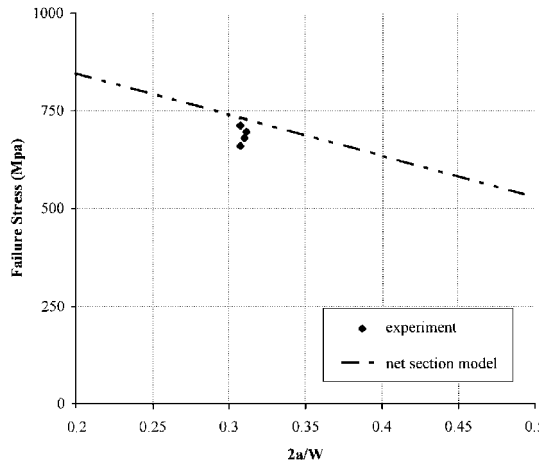

Fig. 10 Failure stress vs flaw size for $[0_2/90_2]_s$ laminate.

unaffected by ply thickness, whereas the notched strength is elevated by increasing the thickness of the plies.

The $[0_n/90_n]_s$ laminate configuration has the 0-deg plies on the outside. This provides less of a constraining effect on the 0-deg plies and makes it easier for the matrix cracks (or axial splits) to grow in the 0-deg layer along the fiber direction. The radiographs of the $[0_2/90_2]_s$ laminate indicate that axial splits and transverse matrix cracks initiate at low levels of the applied load, and the damage zone grows with increasing loads. The axial splits in the 0-deg layer grow to several times the length of the original crack (Fig. 9), and the laminate approaches its net-section strength, as shown in Fig. 10. Final failure is caused by fiber breakage in the 0-deg ply initiating near the crack tip. The $[0_4/90_4]_s$ laminate exhibits a similar damage pattern in the form of transverse matrix cracking in the 90-deg layers, axial splitting in the 0-deg layers, and large delamination zones along the splits at the 0/90 interface. However, laminate failure in this case is induced by delamination along the 0/90 interface, with the surface 0-deg layer completely separating from the adjacent 90-deg layer. This laminate fails at lower stress levels compared to the $[0_2/90_2]_s$ laminate due to the occurrence of a different failure mode. Previous researchers have also observed that thickness and constraint effects play important roles in determining laminate failure modes.[3,6,7]

A comparison of the notched strength response of $[0_2/90_2]_s$ and $[0_2/90_2]_{2s}$ (Figs. 8 and 10) indicates that the $[0_2/90_2]_s$ laminate has higher toughness and approaches the net-section strength, whereas the $[0_2/90_2]_{2s}$ lies in the transition region between a fracture

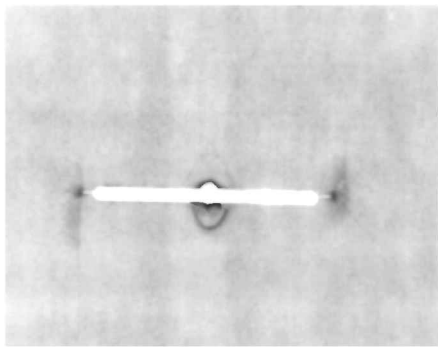

Fig. 11 Crack-tip damage in $[0/90/45/-45]_s$ laminate at 82% of failure load.

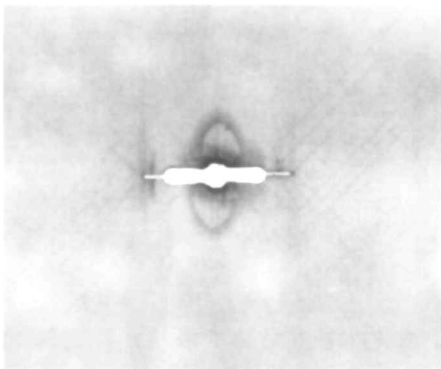

Fig. 12 Crack-tip damage in $[0_2/90_2/45_2/-45_2]_s$ laminate at 86% of failure load.

mechanics controlled failure and net-section type failure. The reason for the difference in notched strength can be attributed to the constraint effect of adjacent 90-deg plies on the interior 0-deg plies of the $[0_2/90_2]_{2s}$ laminate, which inhibits axial split growth in these plies. The resultant higher stress concentration in the interior 0-deg layers controls laminate failure, and these laminates consequently exhibit a lower failure stress than similar configurations consisting of 0-deg plies only on the surface.

Quasi-Isotropic Laminates

Radiographs of typical crack-tip damage in $[0/90/45/-45]_s$ and $[0_2/90_2/45_2/-45_2]_s$ laminates are shown in Figs. 11 and 12, respectively. It can be seen that, unlike the cross-ply laminates, there is no significant change in the dimensions of the damage zone by doubling the ply thickness. The damage zones are also much smaller than those in cross-ply configurations and are localized near the crack tip. As shown in Fig. 13, similar fracture toughness values are also observed for the two laminate configurations, where fracture toughness K_Q is defined as

$$K_Q = Y\sigma_f\sqrt{\pi a} \tag{2}$$

where σ_f is the applied tensile stress at failure, $2a$ is the crack length, and Y is the finite width correction factor.

The similar damage zones and fracture toughness for these laminates seems to indicate that there is little ply thickness effect in these laminates. However, if the ply thickness is further increased, e.g., $[0_4/90_4/45_4/-45_4]_s$ laminate, there is a marked difference in the type of damage, as observed from the radiograph in Fig. 14. Significant amounts of matrix cracking and delamination are observed in the thicker laminate, with the delamination extending to the specimen end tabs at high loads. Ultimate failure of this laminate is induced by delamination along the 0/90 interface. This failure mode occurs at a lower load than the fiber breakage failure mode exhibited by the quasi-isotropic configuration with lower effective ply thickness, and the laminate thus has lower toughness (see Fig. 13). The fracture toughness value for this laminate shown in Fig. 13 represents the stress level at which delamination-induced failure occurs.

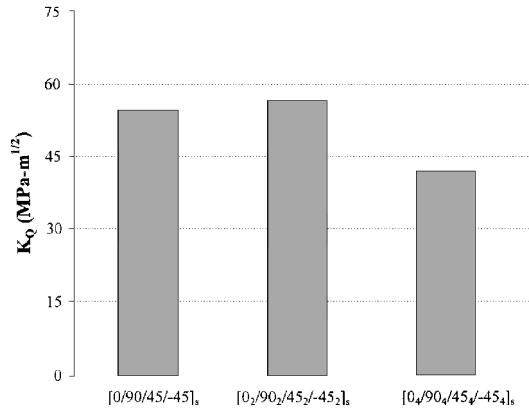

Fig. 13 Fracture toughness of quasi-isotropic laminates.

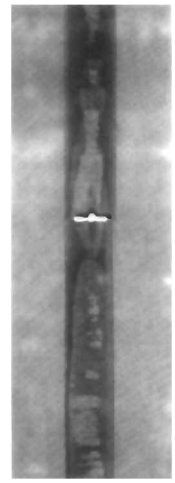

Fig. 14 Damage in $[0_4/90_4/45_4/-45_4]_s$ laminate.

Summary of Experimental Observations

The experimental investigations reveal a significant ply thickness effect in cross-ply laminates. This is caused primarily by the extensive damage zones observed in thicker laminates of this configuration. A large damage zone alleviates the high stresses in the crack-tip region and thereby increases laminate notched strength. As ply thickness increases there is a transition of failure modes from crack-dominated failure to free edge or delamination-induced failure.

The ply thickness effect is less significant in quasi-isotropic laminates, which show little increase in notched strength by doubling the ply thickness. However, if the ply thickness is increased significantly, e.g., four times the nominal thickness, delamination-induced failure occurs at low loads.

Previous results by the authors indicate that non-cross-ply configurations have small damage zones, which are limited to the vicinity of the crack tip.[1] The size of these zones is comparable to those in quasi-isotropic laminates. Because there is little or no ply thickness effect in quasi-isotropic laminates for $n = 1$ and 2, it is reasonable to assume that a similar situation exists for other non-cross-ply laminate configurations as well. For higher values of n, however, different failure modes may come into play and the model may be invalid (as demonstrated in the case of the $[0_4/90_4/45_4/-45_4]_s$ laminate). However, in most composite applications, lumped plies are usually avoided due to their propensity to generate matrix cracks, so the issue of notched response of laminates at high values of n is simply an academic exercise of limited practical significance.

In a previous paper the authors proposed a layup independent failure model to predict the notched strength of fiber-dominated composite laminates.[1] The model parameters were established from tests on configurations with single-ply thickness and did not distinguish between laminates of the same configuration having different ply thickness. The experimental results in this paper indicate that there

is a certain ply thickness effect, and the domain of validity of the proposed model thus must be clarified.

The fracture mechanics based model is based on determining an in situ material parameter that characterizes the fracture toughness of the 0-deg plies in the event of fiber breakage. The model does not explicitly account for the damage-induced stress redistribution near the crack tip. Instead, the effect of any such relaxation is lumped into the effective material parameter. Thus, if a laminate experiences significant crack-tip stress relaxation due to the presence of a large damage zone or fails by a mode other than fiber breakage in the 0-deg plies, it would fall outside the framework of the proposed model. The laminate types in this category include 1) $[0_n/90_n]_s$ laminates, with the 0-deg layer only on the surface, which exhibit large damage zones and approach the net-section strength; 2) $[90_n/0_n/90_n/0_n/90_n]_s$ type laminates (with constrained or interior 0-deg plies) with $n \geq 2$, which exhibit free edge-induced failure and approach net-section strength; and 3) clustered laminate configurations, where failure modes other than fiber breakage in the 0-deg plies could be present, e.g., $[0_n/90_n/45_n/-45_n]_s$ with $n > 2$.

Finite Element Analysis of Crack-Tip Damage

The experimental investigation of failure of notched composite laminates indicates that subcritical damage serves as a mechanism to relax the high stresses in the crack-tip region. The size of this damage zone depends on the type of laminate, with cross-ply laminates typically exhibiting larger damage zones than other configurations considered in this study. It is important to understand the role of such damage on crack-tip stress fields and laminate failure. Moreover, it is important to know when the fracture-mechanics-based criterion becomes invalid because of the presence of crack-tip damage.

These issues are addressed in the present study by conducting a detailed finite element analysis of the problem.

Analysis Procedure

Typical damage in fiber-dominated laminates occurs in the form of axial splitting in the 0-deg ply and delamination, as schematically represented in Fig. 15. This damage is modeled in the present finite element study. The analysis method adopted closely follows the approach developed previously[10] for the study of delamination growth in composites. A commercial code, ABAQUS, is used in the analysis. Because of symmetry about the x, y, and z axes, only one-eight of the specimen is modeled. Figure 16 shows a reduced density

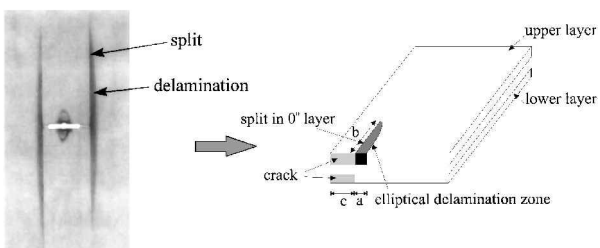

Fig. 15 Schematic of the finite element problem.

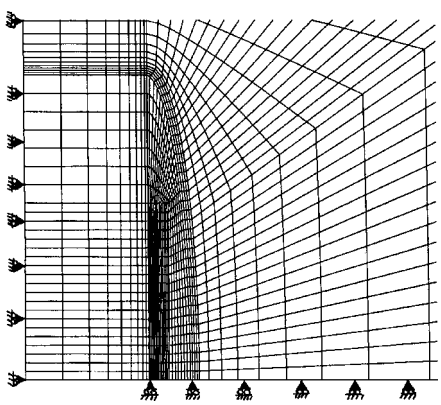

Fig. 16 Reduced density finite element mesh.

finite element mesh modeling the original crack, axial split, and delamination region. The laminate is modeled by two Mindlin plates forming an upper and lower sublaminate. The nodes are located on the mid-planes of each sublaminate. The top layer represents the 0-deg ply of the laminate, whereas the bottom layer represents the other plies.

The matrix crack (axial split) in the top layer is modeled by generating duplicate nodes along the split. Note that the matrix crack exists only in the top layer. Adjacent to the matrix crack is a region of delamination that extends from the tip of the split to the x axis. The shape of the delamination front is modeled by an ellipse, and different delamination fronts can be modeled by varying the aspect ratio b/a of the ellipse. The two-plate model uses approximately 900 elements for each layer (the actual number varies with the delamination aspect ratio), with the smallest element at the split tip about 1/100th of crack length a. Convergence studies indicate that these dimensions are adequate to obtain a converged solution. Constraint equations are imposed on the two plates in the undelaminated region to enforce compatibility along the interface.

The displacement field according to the Mindlin plate theory is as follows:

$$u_x = u_x^0 + z\psi_x, \qquad u_y = u_y^0 + z\psi_y, \qquad u_z = u_z^0 \tag{3}$$

where u, v, and w are the displacement components in the x, y, and z directions; ψ_x and ψ_y are the rotations of the cross sections perpendicular to the x and y axis, respectively; and the superscript refers to displacements at the midplane of the plate.

In the undelaminated region, the upper and lower sublaminates must be tied together in both displacements and rotations along the interface, i.e.,

$$\begin{aligned} u_x^0 - (h/2)\psi_x &= u_x^{0'} + (h'/2)\psi_x' \\ u_y^0 - (h/2)\psi_y &= u_y^{0'} + (h'/2)\psi_y' \\ u_z^0 &= u_z^{0'} \end{aligned} \tag{4}$$

where h represents the sublaminate thickness and the unprimed and primed quantities refer to the upper and lower sublaminates, respectively.

The constraint conditions are input as linear multipoint constraints using the EQUATION command in ABAQUS. The fixed grip loading condition is simulated by constraining the nodes along $y = y_{\max}$ to have the same u_y displacement under an applied load. This is also implemented by using the EQUATION option.

A Fortran code was written to generate the mesh for any split length and delamination aspect ratio. It also generated the ABAQUS input file containing all of the pertinent material definitions, boundary conditions, loading conditions, and information relating to postprocessing the ABAQUS results. The results of the analysis were piped through a Fortran postprocessing program compiled using ABAQUS POST.

The analysis procedure works as follows. First a split length b is assumed, and an elliptical delamination front is modeled with the split as the major axis of the ellipse (the split is assumed to grow with the delamination). Different shapes of the delamination front can be modeled by varying the minor axis a of the ellipse (see Fig. 15). The strain energy release rate for the growth of the split can be calculated by using the modified crack closure technique.[11] In this technique, the strain energy released during crack extension is assumed to equal the work needed to close the open surfaces. The virtual crack extension Δa is usually taken to be small compared to the crack length. Thus, the nodal displacements (crack opening displacements) at the original tip after the extension can be approximated by the nodal displacements (u_i^A and u_i^B) behind the tip before crack extension. The G_{I} and G_{II} for the split extension are given by

$$G_{\mathrm{I}} = [1/(2\Delta a h)]N_x\left(u_x^A - u_x^B\right) + M_y\left(\psi_y^A - \psi_y^B\right) \tag{5}$$

$$G_{\mathrm{II}} = [1/(2\Delta a h)]N_y\left(u_y^A - u_y^B\right) \tag{6}$$

where N and M are the generalized force components at the tip of the split. The presence of the bending terms [second term in Eq. (5)]

implies a variation in G_I through the thickness, but its contribution is negligible compared to the first term.

Effect of Split Length on Stress Distribution in the 0-Degree Layer

A finite element analysis is conducted to study the effect of splitting on the normal stress σ_{yy} in the 0-deg layer along the plane of the notch. A $[0/90]_s$ cross-ply laminate is used in the study. A delamination aspect ratio b/a of 14 is selected, and different lengths of the splits are modeled.

Results of the analysis are plotted in Fig. 17. The solid line represents the situation when there is no split. The σ_{yy} distribution along the x axis for this case follows the theoretical square root singularity. Split initiation removes the singularity, though there still is a region of high-stress concentration near the tip. For small-split lengths (small b/c ratios in Fig. 17), it can be seen that the presence of the split affects the stress distribution only in a small region near the tip. Away from the split tip, the stress distribution seems unaffected by the presence of a split and matches closely with the singular elasticity solution.

Thus, for small-split lengths, the stress field is strongly dominated by the presence of the main crack. As the b/c ratio increases, the stress concentration decreases and approaches a uniform value for very high b/c ratios. This extreme case represents extremely long splits (as are seen in cross-ply laminates), and there is very little stress concentration effect left in the vicinity of the main crack.

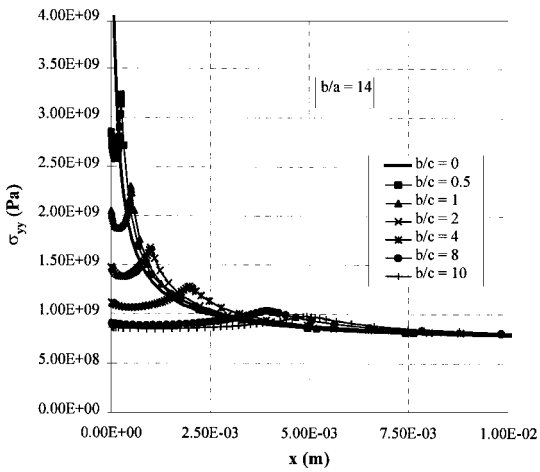

Fig. 17 Effect of split length on stress distribution in the 0-deg layer in $[0/90]_s$ laminate.

Damage Evolution in $[0/90]_{2s}$ Laminates

Subcritical damage in $[0/90]_{2s}$ laminates occurs in the form of long axial splits (matrix cracking) in the surface 0-deg layer, along with delamination between the 0/90 interface. The actual dimensions of the splitting and delamination zone aspect ratio (b/a) are modeled at the measured load levels in the finite element analysis of this problem (Fig. 18). A three-plate model is used in this analysis: the top plate with the split representing the surface 0-deg layer, the middle plate representing the 90-deg layer, and the bottom plate modeled as a layered composite composed of the interior 0- and 90-deg layers. Adjacent plates are connected by imposing the appropriate constraint conditions. The three-plate model is used in this case because it provides a more accurate representation of the constraint on the surface 0-deg layer. No splitting is assumed in the interior 0-deg layer because experimental results indicate that split growth is constrained in interior 0-deg plies. The variation of G_I and G_{II} with the split length is shown in Fig. 19 and presented in Table 2. The results indicate that split growth is controlled by the mode II strain energy release rate G_{II} and seems to occur when the G_{II} at the split tip reaches a constant critical value ($\sim$150 J/m^2).

Results for a similar analysis of damage growth in $[0_2/90_2]_s$ laminates are presented in Table 3, and the variation of G_I and G_{II} with the split length is plotted in Fig. 20. The results indicate that the split growth is controlled by G_{II}, which has a critical value G_{IIcr} approximately equal to 150 J/m^2. Several researchers have investigated the splitting phenomenon of notched unidirectional composites using shear lag type models and have concluded that splitting is controlled by shear (mode II) (Refs. 12–14). A value of 196 J/m^2 for G_{cr} in

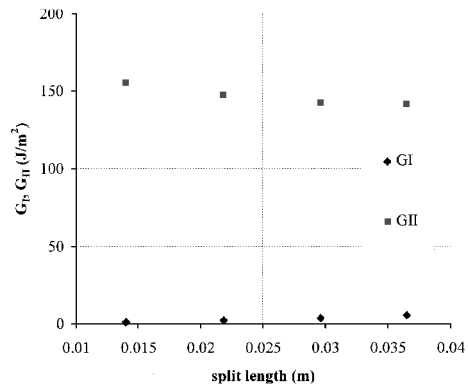

Fig. 19 G_I and G_{II} vs split length for $[0/90]_{2s}$ laminate.

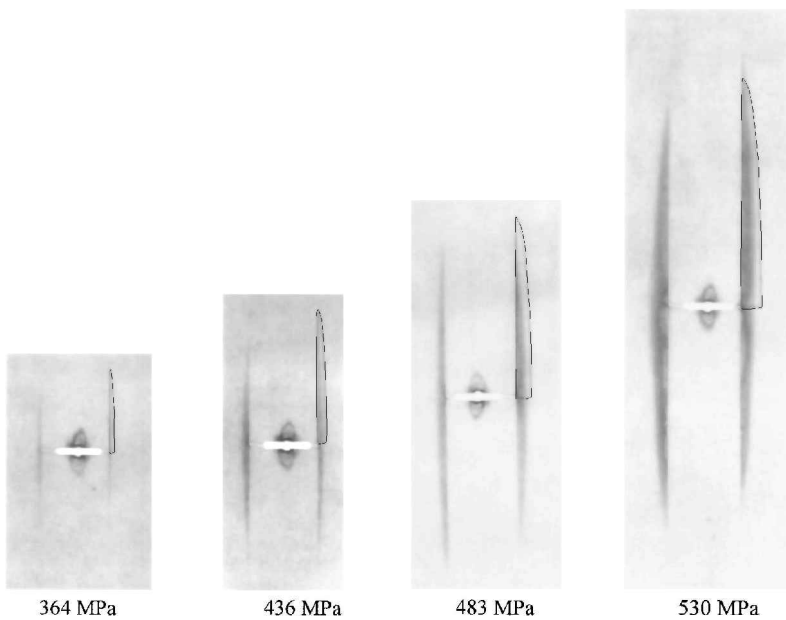

Fig. 18 Damage growth in $[0/90]_{2s}$ laminate modeled using finite element analysis.

Table 2 Variation of G_I and G_{II} of the axial split with loading in $[0/90]_{2s}$ laminate

Applied stress, MPa	Split length b, mm	b/a Ratio	G_I, J/m^2	G_{II}, J/m^2
364	14	18.5	1.27	156
436	21.8	16	2.29	148
483	29.6	13	3.65	142
530	36.5	11.25	5.51	141.5

Table 3 Variation of G_I and G_{II} of the axial split with loading in $[0_2/90_2]_s$ laminate

Applied stress, MPa	Split length b, mm	b/a Ratio	G_I, J/m^2	G_{II}, J/m^2
226	10.3	18	1.29	148
339	22.6	15	2.92	150
449	38	12	6.75	151

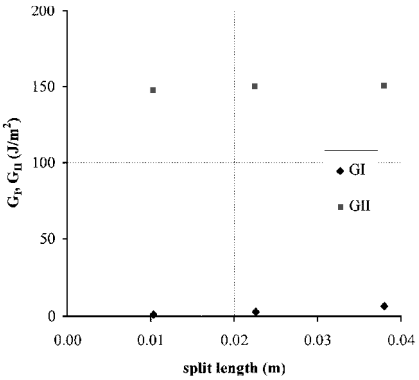

Fig. 20 G_I and G_{II} vs split length for $[0_2/90_2]_s$ laminate.

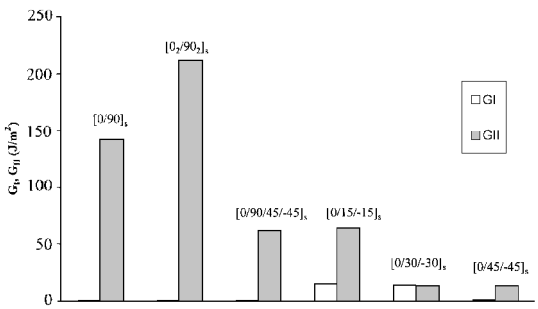

Fig. 21 Effect of laminate layup on G_I and G_{II} of the split in 0-deg layer.

notched unidirectional graphite epoxy laminates has also been reported in the literature.[14]

Effect of Laminate Layup on G_I and G_{II} of the Split

A finite element study was conducted to examine the effect of laminate layup on the strain energy release rates of the split in the 0-deg layer. An elliptical delamination front of aspect ratio $b/a = 14$ was assumed (chosen because this number lies in the range of the experimentally measured delamination aspect ratios). A uniform displacement was prescribed at the y boundary of the mesh to simulate the fixed grip condition. The b/c ratio (split length to half-crack length was chosen as unity). A two-plate model was used to model the cross-ply configurations, whereas a three-plate model was used for the $[0/90/45/-45]_s$ and $[0/\theta/-\theta]_s$ configurations.

Because we want to compare the strain energy release rates at the split of the 0-deg layer in different laminates, the applied loads were chosen so that they all resulted in the same remote stress in the 0-deg layer. The strain energy release rates obtained for the different laminates are plotted in Fig. 21. The following observations can be made from these results.

1) The G_{II} for cross-ply laminates is significantly higher than that for other laminate configurations. Because damage growth seems to occur under a constant G_{IIcr}, these results explain why non-cross-ply laminates have smaller damage zones. The cross-ply laminates provide a weak constraint to the split crack in the 0-deg ply whereas the angle ply laminates provide a stronger constraint.

2) Increasing the ply thickness increases the G_{II} at the tip of the splits in the 0-deg layer of cross-ply laminates. Higher G_{II} values at the same applied load imply that damage can grow farther in laminates with thicker plies. This agrees well with the experimental observation that laminates with greater ply thickness exhibit longer splits and larger damage zones.

Conclusions

The study indicates that the strain energy release rate values for non-cross-ply laminates are small compared to those for cross-ply configurations. This means that the critical damage zone at failure for these laminates would be significantly smaller in non-cross-ply laminates. This conclusion is supported by the experimental observations of the damage zones in different laminate configurations.[1] A smaller damage zone implies that a strong stress concentration exists near the crack tip in the 0-deg layer. As Fig. 17 indicates, for small damage zones, the singular solution is a good approximation of the stress field in the 0-deg layer. Thus, the singular solution would provide a good measure of the local strain energy density associated with fracture. The fracture criterion[1] is based on this singular solution because the critical stress intensity factor of the 0-deg ply is calculated using linear elastic fracture mechanics concepts. The finite element results show that this approximation is valid for small damage zones. Thus, we can conclude that the fracture criterion would work well for fiber-dominated laminates that have small damage zones. Non-cross-ply laminates and well-dispersed cross-ply laminates with interior 0-deg plies fall in this category.

Cross-ply laminates with the 0-deg plies only on the surface or those with clustered configurations show larger damage zones and, thus, would not be accurately predicted by the fracture criterion.[1] Examples of these include the $[0_2/90_2]_s$ laminate, which exhibits net-section type failure, or the $[0_4/90_4]_s$ laminate, which exhibits delamination-induced failure. Alternate failure models are needed to predict the failure of such configurations that lie outside the domain of a fracture mechanics type failure criterion.

Acknowledgments

This work was supported by the Office of Naval Research through Grant N00014-96-1-0822. Y. D. S. Rajapakse was the Grant Monitor.

References

[1]Vaidya, R. S., and Sun, C. T., "Fracture Criterion for Notched Thin Composite Laminates," *AIAA Journal*, Vol. 35, No. 2, 1997, pp. 311–316.

[2]Mandell, J. F., Wang, S. S., and McGarry, F. J., "The Extension of Crack Tip Damage Zones in Fiber Reinforced Composite Laminates," *Journal of Composite Materials*, Vol. 9, 1975, pp. 266–287.

[3]Kortschot, M. T., and Beaumont, P. W. R., "Damage Mechanics of Composite Materials: I—Measurements of Damage and Strength," *Composites Science and Technology*, Vol. 39, 1990, pp. 289–301.

[4]Kortschot, M. T., and Beaumont, P. W. R., "Damage Mechanics of Composite Materials: II—A Damage Based Notched Strength Model," *Composites Science and Technology*, Vol. 39, 1990, pp. 303–326.

[5]Kortschot, M. T., Ashby, M. F., and Beaumont, P. W. R., "Damage Mechanics of Composite Materials: III—Prediction of Damage Growth and Notched Strength," *Composites Science and Technology*, Vol. 40, 1990, pp. 303–326.

[6]Kortschot, M. T., and Beaumont, P. W. R., "Damage Mechanics of Composite Materials: IV—The Effect of Lay-up on Damage Growth and Notched Strength," *Composites Science and Technology*, Vol. 40, 1991, pp. 167–179.

[7]Lagace, P. A., Bhat, N. V., and Gundoglu, A., "Response of Notched Graphite/Epoxy and Graphite/PEEK Systems," *Composite Materials: Fatigue and Fracture*, Vol. 4, ASTM STP 1156, American Society for Testing and Materials, 1993, pp. 55–71.

[8]Harris, C. E., and Morris, D. H., "Effect of Laminate Thickness and Specimen Configuration on the Fracture of Laminated Composites," *Composite Materials: Testing and Design (Seventh Conference)*, ASTM STP 893, American Society for Testing and Materials, 1986, pp. 177–195.

[9]Harris, C. E., and Morris, D. H., "Role of Delamination and Damage Development on the Strength of Thick Notched Laminates," *Delamination and Debonding of Materials*, ASTM STP 876, American Society for Testing and Materials, 1985, pp. 424–447.

[10]Klug, J., Wu, X. X., and Sun, C. T., "Efficient Modeling of Postbuckling Delamination Growth in Composite Laminates Using Plate Elements," *AIAA Journal*, Vol. 34, No. 1, 1996, pp. 178–184.

[11]Jih, C. J., and Sun, C. T., "Evaluation of a Finite Element Based Crack Closure Method for Calculating Static and Dynamic Energy Release Rates," *Engineering Fracture Mechanics*, Vol. 37, No. 2, 1990, pp. 313–322.

[12]Nairn, J. A., "Fracture Mechanics of Unidirectional Composites Using the Shear-Lag Model I: Theory," *Journal of Composite Materials*, Vol. 22, 1988, pp. 561–588.

[13]Dharani, L. R., and Recker, R. L., "Growth of Longitudinal Matrix Damage in Unidirectional Composites," *Engineering Fracture Mechanics*, Vol. 38, No. 2/3, 1991, pp. 185–195.

[14]Nairn, J. A., Liu, S., and Chen, H., "Longitudinal Splitting in Epoxy and K-Polymer Composites: Shear Lag Analysis Including the Effect of Fiber Bridging," *Journal of Composite Materials*, Vol. 25, 1991, pp. 1086–1107.

G. A. Kardomateas
Associate Editor